ELSEVIER

Journal of Nuclear Materials 307–311 (2002) 536–539

journal of nuclear materials

www.elsevier.com/locate/jnucmat

On the mechanical properties of the advanced martensitic steel EUROFER 97

P. Spätig [a,*], G.R. Odette [b], G.E. Lucas [b], M. Victoria [a]

[a] *Fusion Technology, Centre de Recherches en Physique des Plasmas, Ecole Polytechnique Fédérale de Lausanne, CH-5232 Villigen PSI, Switzerland*

[b] *Department of Mechanical and Environmental Engineering, University California, Santa Barbara, CA 93106-5080, USA*

Abstract

In an effort to better understand the plasticity of tempered martensitic steels, uniaxial tension and compression tests were carried out. The temperature dependence of both the yield stress and the post-yield stress behavior were compared, and it was shown that a good correspondence exists between tensile and compressive behavior. The strain-hardening of EUROFER 97 steel was examined in terms of dislocation mechanics. A simple strain-hardening law was established within the framework of a model accounting for dislocation storage and annihilation. Moreover, an analytical constitutive equation was derived which describes the overall post-yield curve. While the equation predicts the flow stress should reach a saturation stress with strain, this could not be verified by the mechanical tests due to deformation instabilities such as necking in tension or side-slip buckling in compression. Additional tests will have to be devised and applied to investigate these predictions.

1. Introduction

This study was performed as part of an international investigation on the 7–9Cr tempered martensitic steels, which are among the main candidate structural materials for the first wall and blanket of commercial fusion reactors [1]. We report on the mechanical properties investigated by uniaxial tension and compression tests of the European tempered martensitic steel EUROFER 97. The objectives are several. First, the results presented are motivated by the need for a better understanding of the plasticity of tempered martensitic steels. The relationship between the constitutive behavior and the initial microstructure as well as its evolution with strain still requires in-depth investigations. Second, the tensile properties are often related to other mechanical properties determined by using more complex modes of loading. For instance, hardness testing obtained from ball indenters imposes a multiaxial loading state (e.g. [2,3]). One goal of this paper is to verify whether the tensile and compressive properties are similar enough to be considered interchangeable. Finally it is of interest to establish the overall constitutive behavior with compression tests on irradiated materials. On the one hand, this would permit the study of deformation to strain levels much higher than those reachable by tensile testing due to necking instability. On the other hand, when fracture toughness studies are undertaken, it is quite reasonable to envisage extracting small compression specimens from tested fracture specimens to locally assess the constitutive behavior of a given specimen. Thus material variability and/or inhomogeneities in irradiation temperature or fluence within a capsule could be tracked.

This paper aims only at presenting preliminary results on the differences and similarities of mechanical properties obtained in compression and tension of an advanced tempered martensitic steel. Efforts have also been made to model the post-yield behavior; but, due to space limitations, a more detailed description of the modeling of the constitutive behavior in relation to the

* Corresponding author. Tel.: +41-56 310 2934; fax: +41-56 310 4529.

E-mail address: philippe.spatig@psi.ch (P. Spätig).

0022-3115/02/$ - see front matter
PII: S0022-3115(02)01213-8

initial dislocation structure and its evolution is given elsewhere [4].

2. Experimental

The alloy in this study is the reduced activation EUROFER 97 steel, heat E83697, produced by Böhler AG. This steel contains 8.90 wt% Cr, 0.12 wt% C, 0.46 wt% Mn, 1.07 wt% W, 0.2 wt% V, 0.15 wt% Ta and Fe for the balance. The steel was heat-treated by normalizing at 1253 K for 0.5 h and tempering at 1033 K for 1.5 h. The steel was fully martensitic after quenching. The prior austenite grain size was about 10 (ASTM) [5].

Tensile tests were performed on round specimens 3 mm in diameter and 18 mm in gauge length. The tests were carried out on an electro-mechanical RMC100 Schenck machine at constant piston velocity corresponding to a nominal strain rate of 5×10^{-4} s^{-1} at 293, 423 and 623 K under vacuum. Compression tests were performed with cylindrical specimens 3 mm in diameter and 5.5 mm in length on another RMC100 Schenck machine under the same nominal strain rate and temperatures as those of the tensile tests, but under a helium environment. The stresses, σ and strains, ε, reported in this paper are the true stresses and true strains.

3. Results and discussion

The yield stresses, $\sigma_{0.002}$, measured at a plastic strain $\varepsilon_p = 0.002$ are plotted in Fig. 1. The yield stresses determined in compression were found to be slightly, but systematically lower than those in tension. While the largest difference (29 MPa) was obtained at room temperature, this difference represents less than 6% of the

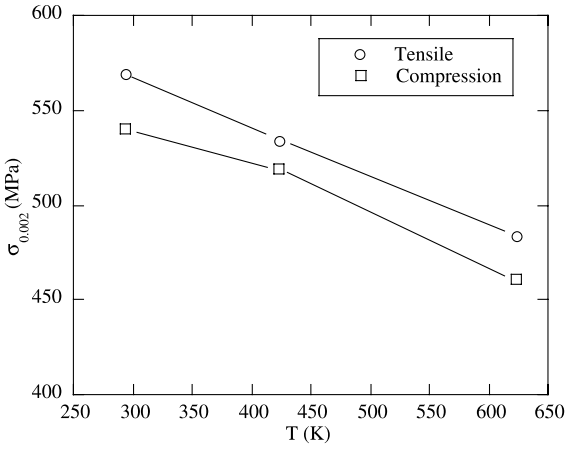

Fig. 1. Temperature dependence of $\sigma_{0.002}$ in tensile and compression mode.

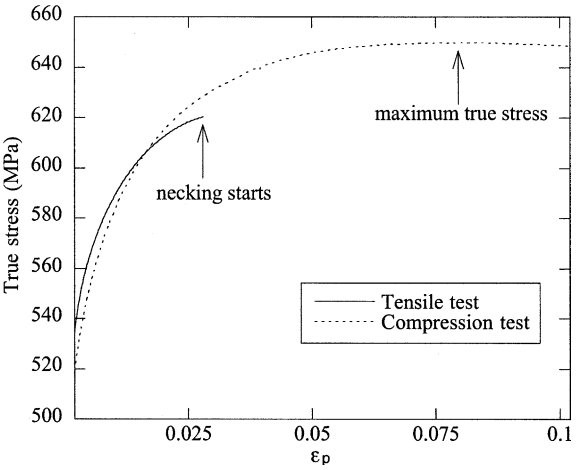

Fig. 2. Deformation curve σ–ε_p at 423 K in tensile and compression mode.

absolute value of the yield stress. Thus, it can be considered that $\sigma_{0.002}$ in both deformation modes are reasonably comparable.

The post-yield behavior was studied as follows. As an example of the comparative stress–strain behavior in tension and compression, Fig. 2 shows the results of two tests performed at 423 K. For the tensile test, the deformation curve is plotted only up to the strain at which necking starts. The overall shapes of the two curves look quite similar to one another, with a parabolic type of strain-hardening previously observed for this kind of steel [6,7]. A significantly larger strain was obtained for the compression test, and a maximum true stress of 650 MPa was attained at $\varepsilon_p = 0.8$. After testing, observations of the deformed specimen shape revealed that the specimen underwent a slight side-slip buckling as described in [8]. For this reason and in the following, we analyzed only the beginning of the compression curve up to 5% of plastic strain to avoid incorporating the above mentioned compression instability into the analysis of the strain-hardening. The post-yield behavior was then investigated by decomposing the total flow stress into the yield stress and a post-yield component as

$$\sigma(\varepsilon, \dot{\varepsilon}, T) = \sigma_y(\dot{\varepsilon}, T) + \sigma_{pl}(\varepsilon, \dot{\varepsilon}, T). \quad (1)$$

The strain-hardening is defined as $d\sigma/d\varepsilon_p = d\sigma_{pl}/d\varepsilon_p$. Investigations of the strain-hardening for this class of steel have been performed previously [6,7]. However, it has not been possible so far to establish an integrated relationship between the stress and strain for the whole deformation curve from the yield stress up to the necking instability in the case of tensile testing. In a recent study [9], strain-hardening analysis was performed by using the total dislocation density equation evolution with strain, based on the storage and annihilation of

dislocations. It is well known that the storage probability of a dislocation is inversely proportional to an effective mean free path L_{eff} (e.g. [10]). Assuming that different processes acting in parallel limit the mean free path of the dislocations, the inverse of L_{eff} is the sum of the inverse mean free paths of each process. In [9], we made the assumption that L_{eff} was the result of two mechanisms occurring in parallel. The first one was associated with the mean free path prescribed by the cell size, which can be considered as the lath size for tempered martensitic steels. The second one was related to the average spacing between the dislocations; this spacing being proportional to $\rho^{1/2}$. The annihilation term was taken to be proportional to the total dislocation density. With the previous hypotheses, a strain-hardening law could be obtained that was found to describe properly the calculated strain-hardening versus stress.

Motivated by the search for a compact integrated relationship between σ_{pl} and ε_{p}, we assumed hereafter that the storage process associated with the lath size is the dominant one so that the mean free path is taken as the average lath size D. In this case, the dislocation density evolution can be written as, [11,12]

$$\frac{\mathrm{d}\rho}{\mathrm{d}\varepsilon_{\text{p}}} = \frac{\mathrm{d}\rho^{+}}{\mathrm{d}\varepsilon_{\text{p}}} + \frac{\mathrm{d}\rho^{-}}{\mathrm{d}\varepsilon_{\text{p}}} = M(k_1 - k_2\rho), \tag{2}$$

where k_1, determined by a constant mean free path D, is equal to $(bD)^{-1}$, $k_2\rho$ accounts for the dynamic annihilation of dislocations and M is the Taylor factor. Considering that σ_{pl} arises from an increase of stored dislocations and represents dislocation–dislocation interaction, σ_{pl} is then related to the total dislocation density ρ by the usual equation:

$$\sigma_{\text{pl}} = M\alpha Gb\sqrt{\rho}, \tag{3}$$

where α is dimensionless constant, G is the shear modulus, b is the amplitude of the Burgers vector and ρ is the total dislocation density. Using the definition of the strain-hardening $\mathrm{d}\sigma_{\text{pl}}/\mathrm{d}\varepsilon_{\text{p}}$ and Eqs. (2) and (3) above, the strain-hardening as a function of stress becomes

$$\mathrm{d}\sigma_{\text{pl}}/\mathrm{d}\varepsilon_{\text{p}} = \theta_{\text{p}}(\sigma_{\text{pl}}) = \frac{P_1}{\sigma_{\text{pl}}} - P_2\sigma_{\text{pl}}. \tag{4}$$

P_1 and P_2 are equal to $M^3(\alpha G)^2 b/2D$ and $Mk_2/2$, respectively. The last equation can be analytically integrated to obtain

$$\sigma_{\text{pl}} = \sqrt{\frac{P_1 - (P_1 - P_2\sigma_{\text{pl},i}^2)\exp(-2P_2(\varepsilon_{\text{p}} - \varepsilon_{\text{p},i})}{P_2}}. \tag{5}$$

The origin of the σ_{pl} was chosen at $\varepsilon_{\text{p},i} = 0.001$, at which $\sigma_{\text{pl}} = \sigma_{\text{pl},i}$ and the analysis of the curves which follow was done from $\varepsilon_{\text{p}} = 0.002$. It is worth noting here that in Eq. (5) as ε_{p} tends to infinity, σ_{pl} approaches a saturation stress, σ_{sat}, that is equal to $(P_1/P_2)^{1/2}$. Fig. 3 shows the fit

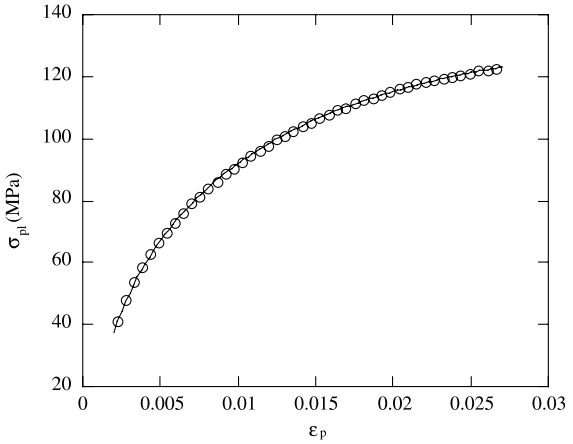

Fig. 3. σ_{pl}–ε_{p} with fit as Eq. (5).

to Eq. (5) of experimental data at 423 K for a tensile test. Fits of that quality were obtained at the other investigated temperatures and also for the compression deformation conditions. In order to pursue the comparison between tension and compression, we report the temperature dependence in Figs. 4 and 5 of the parameters P_1 and P_2 and σ_{sat}, respectively. It can be seen that the parameters P_1 and P_2 follow the same trend with temperature for both deformation modes. P_1 exhibits a slight decrease above 450 K while P_2 clearly increases, reflecting the thermally activated nature of the dynamics of annihilation of dislocations. Interestingly, neither significant nor systematic discrepancies are observed between the values of P_1 and P_2 obtained in compression and in tension. The temperature dependence of the saturation stress of σ_{pl} defined by $(P_1/P_2)^{1/2}$ shows a monotonic decrease from about 200 MPa at room temperature down to 100 MPa at 623 K. This decrease is

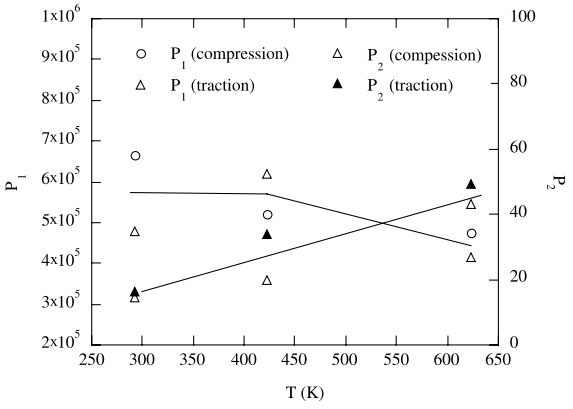

Fig. 4. Temperature dependence of the strain-hardening parameters P_1 and P_2.

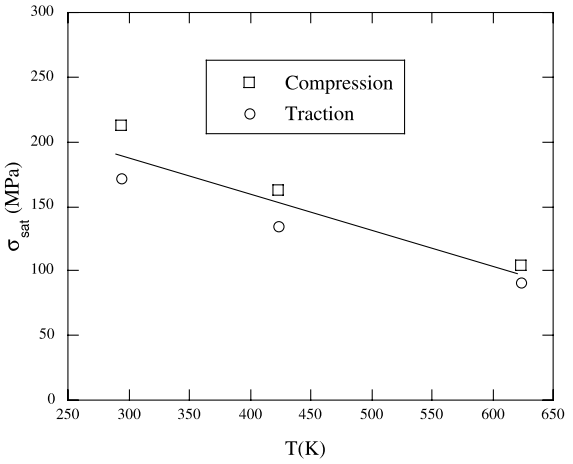

Fig. 5. Temperature dependence of the saturation stress.

the direct consequence of the increase of P_2 as discussed above.

4. Summary

A series of tension and compression tests was undertaken on the advanced tempered martensitic steel EUROFER 97 between 293 and 623 K. The yield stress and strain-hardening parameters obtained from both deformation modes show quite comparable values as well as similar temperature dependencies. The strain-hardening law is based on a dislocation dynamics model taking into account the storage and annihilation of the dislocations. For the storage term, the mean free path of the dislocations is prescribed by the lath size and is considered constant to a first approximation. The dynamic annihilation is assumed to be linear with total dislocation density. The strain-hardening law was integrated to yield a new analytical relationship between the plastic component of the flow stress and the plastic strain, allowing construction of the whole tensile curve from the yield point up to necking. Similarly, the compression deformation curves could be reconstructed but up to a larger strain level with the same relationship. A saturation stress is predicted by this analytical constitutive relation that could not be reached during the compression because side-slip buckling was observed to occur before the predicted saturation stress was reached. Additional tests will have to be devised and applied to further investigate this.

Acknowledgements

The financial support of EURATOM is gratefully acknowledged. The Paul Scherrer Institute is acknowledged for the overall use of facilities. The compression testing was performed at the Physics Department-EPFL in the group of Professor J.-L. Martin who put his testing machine to our disposal. Dr Kruml is thanked for his help in the compression testing.

References

[1] B. van der Schaaf, D.S. Gelles, S. Jitsukawa, A. Kimura, R.L. Klueh, A. Möslang, G.R. Odette, J. Nucl. Mater. 283–287 (2000) 52.
[2] F.M. Haggag, in: W.R. Corwin, F.M. Haggag, W.L. Server (Eds.), ASTM STP 1204, ASTM, Philadelphia, PA, 1993, p. 27.
[3] S.-H. Song, R.G. Faulkner, P.E.J. Flewitt, R.F. Smith, P. Marmy, Mater. Sci. Eng. A 281 (2000) 75.
[4] P. Spätig, R. Schäublin, M. Victoria, to be published.
[5] H.E. Hofmans, NRG Reports 20023/00.38153/P, 2000.
[6] P. Spätig, G.R. Odette, E. Donahue, G.E. Lucas, J. Nucl. Mater. 283–287 (2000) 721.
[7] P. Spätig, N. Baluc, M. Victoria, Mater. Sci. Eng. A 309–310 (2001) 425.
[8] Mechanical Testing, ASM Handbook, Vol. 8, 1992, p. 55.
[9] P. Spätig, R. Schäublin, M. Victoria, in: H.M. Zbib, G.H. Campbell, M. Victoria, D.A. Hughes, L.E. Levine (Eds.), Material Instabilities and Patterning in Metals, Mater. Res. Soc. Symp. Proc. 683E (2001) B1.10.1.
[10] D.J. Bammann, Mater. Sci. Eng. A 309–310 (2001) 406.
[11] Y. Estrin, H. Mecking, Acta Metal. 32 (1) (1984) 57.
[12] M. Verdier, Y. Bréchet, P. Guyot, Acta Mater. 47 (1999) 127.